

Numerical Prediction of Natural Convection Phenomena Through a Square Enclosure with a Heated Circular Cylinder at Different Horizontal Locations

Salam Hadi Hussain

University of Babylon/College of Engineering/Mechanical Engineering Department

Mohsen Gawy Hamza

Al-Qadisiya University/College of Engineering/Mechanical Engineering Department

Abstract

In this paper, numerical simulations are carried out for natural convection induced by a temperature difference between a heated circular cylinder and a cold outer square enclosure. A two dimensional Navier-Stokes equation is solved by using finite volume discretization with SIMPLE algorithm in non-orthogonal body-fitted coordinate system. Detailed flow and heat transfer features for different Rayleigh numbers varying over the range 10^3 - 10^6 are reported. The study goes further to investigate the effect of the inner cylinder location on the heat transfer and fluid flow. The location of the inner circular cylinder is changed horizontally along the center-line of square enclosure with δ (-0.25L to 0.25L). The size, number and formation of the vortices and shape of thermal plume strongly depend on the Rayleigh number and the position of the inner circular cylinder. Overall heat transfer also changes for different position of the inner circular cylinder. The results showed a good agreement with another published results.

Keywords: Finite volume, Natural convection, Square enclosure, Heated inner cylinder

الخلاصة

في الدراسة الحالية، أجريت محاكاة عددية للحمل الحر الناتج من الفرق الحراري بين اسطوانة داخلية مسخنة محاطة بحيز بارد مربع الشكل. ولغرض حل هذه المسألة تم استخدام معادلات نافير-ستوك ثنائية الأبعاد حيث حلت هذه المعادلات باستخدام طريقة الحجم المحددة مع النموذج المبسط (SIMPLE algorithm) مع نظام غير متعامد متطابق مع حدود الجسم. قامت الدراسة بالوصف المفصل للحرارة والجريان لأعداد رالية من 10^3 - 10^6 وقد تم استقصاء تأثير موقع الاسطوانة الداخلية على انتقال الحرارة وجريان المائع حيث إن موقع الاسطوانة الدائرية الداخلية يتغير بشكل أفقي وعلى خط المركز للحيز المغلق المربع حيث كان مقدار التغير الأزاحي يتراوح بين (-0.25L إلى 0.25L). توصلت الدراسة إلى أن حجم وعدد وشكل الدوامات والأثر الحراري يعتمد بشكل كبير على أعداد رالية وموقع الاسطوانة الداخلية وكذلك الحرارة الكلية المنتقلة تتغير للمواقع المختلفة للاسطوانة الداخلية. النتائج أوضحت تطابق جيد مع النتائج الأخرى المنشورة.

Nomenclature:

Symbol	Description	Unit
a_1, a_2	Transformation coefficients	
F	Control function	
g	Gravitational acceleration	m/s^2
J	Jacobian of residual equations	
k	Thermal conductivity	$W/m \cdot ^\circ C$
L	height of the square enclosure	m
n	Normal direction to the wall	
Nu	Local surface Nusselt number	
\overline{Nu}	Average surface Nusselt number	
P	Dimensionless pressure	
p	Pressure	N/m^2
Pr	Prandtl number	
Q	Control function	

Ra	Rayleigh number	
R	Radius of circular cylinder	m
S_N	Source term due to non orthogonal characteristic of grid system	
S_ϕ	<i>Linearized source term for ϕ</i>	
T	Temperature	°C
T_h	High temperature	°C
T_c	Low temperature	°C
U	Dimensionless velocity component in x-direction	
u	Velocity component in x-direction	m/s
V	Dimensionless velocity component in y-direction	
v	Velocity component in y-direction	m/s
X	Dimensionless Coordinate in horizontal direction	
x	Cartesian coordinate in horizontal direction	m
Y	Dimensionless Coordinate in vertical direction	
y	Cartesian coordinate in vertical direction	m
W	Surface area of walls	
Greek Symbols		
α	Thermal diffusivity	m^2/s
β	Volumetric coefficient of thermal expansion	K^{-1}
ϕ	Variable vector	
Γ_ϕ	Diffusion coefficient for parameter	
θ	Dimensionless temperature	
δ	Distance from center of the square cylinder to circular cylinder center	m
ν	Kinematic viscosity of the fluid	m^2/s
ρ	Density of the fluid	kg/m^3
ξ, η	Dimensionless body-fitted coordinates	

1. Introduction

Natural convection in enclosures has been considerable interest in many industrial and science applications, for example, collection of solar energy, operation and safety of nuclear reactors, electric devices and stratified atmospheric boundary layers. In engineering applications, the geometries that arise, however, are more complicated than a simple enclosure filled with a convective fluid. The geometric configuration of interest is with the presence of bodies embedded with the enclosure. (Lacroix, 1992; Ghaddar and Thiele, 1994; Saha, 2000; Ding et al., 2005; and Kim et al., 2008) .

Buoyancy driven flow and heat transfer between a cylinder and its surrounding medium has been a problem of considerable importance. This problem has a wide range of applications. Energy storage devices, crude oil storage tanks, heat exchangers, spent fuel storage of nuclear power plants are a few to name. Ghaddar, 1992, reported the numerical results of natural convection from a uniformly heated horizontal cylinder placed in a large air-filled rectangular enclosure. He observed that flow and the thermal behaviors depend on heat fluxes imposed on the inner cylinder within the isothermal enclosure. He also obtained a correlation of the average Nusselt number as a function of Rayleigh number.

Moukalled and Acharya, 1996, studied the change of the thermo-flow field between the low temperature outer square enclosure and high temperature inner circular cylinder according to the radius of the inner circular cylinder. They considered three different aspect ratio, r/L of the cylinder radius, r to the enclosure height, L in the range of Rayleigh numbers from 10^4 to 10^7 . They showed that, at a constant enclosure aspect

ratio, the total heat transfer increases with increasing Rayleigh number. When the Rayleigh number is constant, the convection contribution to the total heat transfer decreases with increasing aspect ratio value.

Sasaguchi et al.,1998, reported the numerical results of the effect of the position of a cooled cylinder in a rectangular cavity on the cooling process of water around the cylinder. The initial water temperature is varied at 4,6,8 and 12 °C, while the temperature of the cylinder surface is fixed at 0 °C. They observed that the changes in the position of the cylinder and the initial water temperature largely affect on fluid flows. Also, they found that the average Nusselt number over the cylinder surface and averaged water temperature vary in a complicated manner with time for initial water temperature greater than 4°C. The cooling rate of water is largely affected by the change of the position of the cylinder.

Cesini et al.,1999, performed the numerical and experimental analysis of natural convection from a horizontal cylinder enclosed in a rectangular cavity. The influence of the cavity aspect ratio and the Rayleigh number on the distribution of temperature and Nusselt number was investigated. As a result, the average heat transfer coefficients increases with increasing Rayleigh number.

Asan, 2000, investigated numerically the two dimensional natural convection flow in an annulus between two isothermal concentric square ducts and obtained solutions up to a Rayleigh number of 10^6 . The results showed that dimension ratio and Rayleigh number have a profound influence on the temperature and flow field.

Shu et al., 2000, presented a numerical study of natural convection between an outer square enclosure and inner circular cylinder according to the eccentricity and angular position of the inner circular cylinder at a Rayleigh number of 3×10^5 . They found that the global circulation, flow separation and the top space between the square outer enclosure and circular inner cylinder have significant effects on the plume inclination.

Shu and Zhu, 2002, obtained the numerical results for Rayleigh numbers ranging from 10^4 to 10^6 and aspect ratios between 1.67 and 5.0. It was found that both the aspect ratios and the Rayleigh number are critical to the patterns of flow and thermal fields, also, they suggested that a critical aspect ratios may exist at high Rayleigh numbers to distinguish the flow and thermal patterns.

Kumar De and Dalal, 2006, considered the problem of natural convection around a square, horizontal, heated cylinder placed inside an enclosure in the range of Rayleigh numbers from 10^3 - 10^6 . Effects of the enclosure geometry have been assessed using three different aspect ratios placing the square cylinder at different heights from the bottom. As a results, it was found that the uniform wall temperature heating is quantitatively different from the uniform wall heat flux heating. The flow pattern and thermal stratification were modified, if the aspect ratio was varied. Overall heat transfer also changes as a function of aspect ratio.

Kim et al., 2008, considered the problem of natural convection around a horizontal circular cylinder placed inside an enclosure in the range of Rayleigh numbers from 10^3 - 10^6 . The location of the inner circular cylinder is changed vertically along the center line of square enclosure. They found the number, size and formation of the vortex strongly depend on the Rayleigh number and the position of the inner circular cylinder. As a results, the changes in heat transfer quantities have also depend on the Rayleigh number and location of the inner cylinder.

In the present study the natural convection around heated circular cylinder inside a square enclosure with different horizontal location is investigated numerically by using finite volume method. The purpose of the present study is to examine how the position

of the inner circular cylinder relative to the outer square cylinder affects on the natural convection phenomena for different Rayleigh numbers.

2. Mathematical Analysis:

A schematic of the system considered in the present study is shown in Fig. 1. The system consists of a square enclosure with sides of length L , within which a circular cylinder with a radius R ($= 0.2 L$) is located and moves along the horizontal centerline in the range from $-0.25 L$ to $0.25 L$. The walls of the square enclosure was kept at a constant low temperature of T_c , whereas the inner circular cylinder was kept at a constant high temperature of T_h . The present work is based on the previous work by Kim et al., 2008, but in their work attention has been considered to investigate the effect of inner heated cylinder with vertical location placed inside a square enclosure on the heat transfer and fluid flow. The present work deals with same problem but in this situation, the flow and heat transfer in the enclosure are investigated along the horizontal location of the inner circular cylinder for different Rayleigh numbers. The purpose of the present study is to examine how the position of the inner circular cylinder relative to the outer square cylinder affects on the natural convection phenomena for different Rayleigh numbers when a hot inner circular cylinder is located at different positions along the horizontal centerline of the outer square cylinder. In the simulations to be reported here the Prandtl number, Pr , and R have been taken to be 0.7 corresponding to that of air and 0.2, respectively. The Rayleigh number, Ra , varies in the range of 10^3-10^6 . The dimensionless horizontal distance δ , which represents the position of the inner cylinder along the horizontal centerline, varies in the range of $-0.25 L$ to $0.25 L$. The results are presented in terms of an isotherms and a stream lines graphs.

The fluid properties are also assumed to be constant, except for the density in the buoyancy term, which follows the Boussinesq approximation. The gravitational acceleration acts in the negative y -direction. The fluid inside the square enclosure is assumed Newtonian while viscous dissipation effects are considered negligible. The viscous incompressible flow and the temperature distribution inside the square enclosure with a circular cylinder are described by the Navier–Stokes and the energy equations, respectively. The governing equations are transformed into a dimensionless forms under the following non-dimensional variables [Kim et al., 2008]:

$$\theta = \frac{T - T_c}{T_h - T_c}, X = \frac{x}{L}, Y = \frac{y}{L}, U = \frac{uL}{\alpha}, V = \frac{vL}{\alpha},$$

$$P = \frac{pL^2}{\rho\alpha^2}, Pr = \frac{\nu}{\alpha} \text{ and } Ra = \frac{g\beta(T_h - T_c)L^3 Pr}{\nu^2} \quad (1)$$

where X and Y are the dimensionless coordinates measured along the horizontal and vertical axes, respectively, u and v being the dimensional velocity components along x and y axes, and θ is the dimensionless temperature. β is the volumetric coefficient of thermal expansion and g is the gravitational acceleration. The dimensionless forms of the governing equations under steady state condition are expressed in the following forms [Kim et al., 2008]:

$$\frac{\partial U}{\partial X} + \frac{\partial V}{\partial Y} = 0$$

$$U \frac{\partial U}{\partial X} + V \frac{\partial U}{\partial Y} = -\frac{\partial P}{\partial X} + Pr \left(\frac{\partial^2 U}{\partial X^2} + \frac{\partial^2 U}{\partial Y^2} \right) \quad (3)$$

$$U \frac{\partial V}{\partial X} + V \frac{\partial V}{\partial Y} = -\frac{\partial P}{\partial Y} + Pr \left(\frac{\partial^2 V}{\partial X^2} + \frac{\partial^2 V}{\partial Y^2} \right) + RaPr\theta \quad (4)$$

$$U \frac{\partial \theta}{\partial X} + V \frac{\partial \theta}{\partial Y} = \left(\frac{\partial^2 \theta}{\partial X^2} + \frac{\partial^2 \theta}{\partial Y^2} \right) \quad (5)$$

The rate of heat transfer is computed at each wall and is expressed in terms of local surface Nusselt number (Nu) and surface-averaged Nusselt number (\overline{Nu}) as [Arpaci and Larsen, 1984]:

$$Nu = \frac{\partial \theta}{\partial n} \Big|_{wall} ,$$

Where n is the normal direction with respect to the walls, W is the surface area of walls.

3. Numerical Analysis:

The grid generation calculation is based on the curvilinear coordinate system applied to fluid flow as described by Thompson et al., 1974. Fig. (2) shows the schematic of two dimensions body fitting grid used for the present computation. This grid was obtained by solving non homogeneous 2-D Poisson equations [Thomas and Middlecoff, 1980] :

$$\left. \begin{aligned} \xi \xi_{xx} + \xi \xi_{yy} &= F(\xi, \eta) \\ \eta \eta_{xx} + \eta \eta_{yy} &= Q(\xi, \eta) \end{aligned} \right\} \quad (7-a)$$

Define F and Q in the following formulae,

$$F = \frac{1}{h_1 h_2} f_\xi \quad \text{and} \quad Q = \frac{1}{h_1 h_2} \left(\frac{1}{f} \right)_\eta \quad (7-b)$$

Where

$$h_1 = g_{11}^{\frac{1}{2}} \quad \text{and} \quad h_2 = g_{22}^{\frac{1}{2}} \quad (7-d)$$

$$f = \frac{h_2}{h_1} = \left(\frac{x_\eta^2 + y_\eta^2}{x_\xi^2 + y_\xi^2} \right)^{\frac{1}{2}} \quad (7-e)$$

$$f_\xi = \frac{\left(\frac{x_\eta^2 + y_\eta^2}{x_\xi^2 + y_\xi^2} \right)^{\frac{1}{2}} (x_\eta x_{\eta\xi} + y_\eta y_{\eta\xi}) - \left(\frac{x_\eta^2 + y_\eta^2}{x_\xi^2 + y_\xi^2} \right)^{\frac{1}{2}} (x_\xi x_{\xi\xi} + y_\xi y_{\xi\xi})}{x_\xi^2 + y_\xi^2} \quad (7-f)$$

$$\left(\frac{1}{f}\right)_\eta = \frac{\left(\frac{x_\eta^2 + y_\eta^2}{x_\xi^2 + y_\xi^2}\right)^{\frac{1}{2}} (x_\xi x_{\eta\xi} + y_\xi y_{\eta\xi}) - \left(\frac{x_\xi^2 + y_\xi^2}{x_\eta^2 + y_\eta^2}\right)^{\frac{1}{2}} (x_\eta x_{\eta\xi} + y_\eta y_{\eta\xi})}{x_\eta^2 + y_\eta^2} \quad (7-g)$$

where F and Q are control functions used to clustering the grid near the walls to sense the velocity gradient because there is a friction between the wall and the fluid. Equations (7) are transformed to (ξ, η) coordinates by interchanging the roles of dependent variables, this yield the following system equations [Thomas and Middlecoff, 1980]:

$$\left. \begin{aligned} \mathbf{g}_{11}\mathbf{x}_{\xi\xi} - \mathbf{g}_{21}\mathbf{x}_{\xi\eta} + \mathbf{x}_{\eta\eta} &= -\mathbf{J}^2 (\mathbf{F}\mathbf{x}_\xi + \mathbf{Q}\mathbf{x}_\eta) \\ \mathbf{g}_{11}\mathbf{y}_{\xi\xi} - \mathbf{g}_{21}\mathbf{y}_{\xi\eta} + \mathbf{y}_{\eta\eta} &= -\mathbf{J}^2 (\mathbf{F}\mathbf{y}_\xi + \mathbf{Q}\mathbf{y}_\eta) \end{aligned} \right\} \quad (8-a)$$

Where;

$$\mathbf{g}_{11} = x_\eta^2 + y_\eta^2 \quad (8-b)$$

$$\mathbf{g}_{21} = 2 (x_\xi x_\eta + y_\xi y_\eta) \quad (8-c)$$

$$\mathbf{g}_{22} = x_\xi^2 + y_\xi^2 \quad (8-d)$$

$$\mathbf{J} = x_\xi y_\eta - x_\eta y_\xi \quad (8-e)$$

Using centered difference scheme to discretize the equation (8-a) we obtain:

$$\begin{aligned} x_{i,j}^n &= \frac{\hat{\alpha}}{2(\hat{\alpha} + \hat{\gamma})} (x_{j-1,i} + x_{j+1,i}) + \frac{\hat{\gamma}}{2(\hat{\alpha} + \hat{\gamma})} (x_{j,i-1} + x_{j,i+1}) + \\ &\frac{0.5 \hat{\delta}}{2(\hat{\alpha} + \hat{\gamma})} F(x_{j+1,i} - x_{j-1,i}) + \frac{0.5 \hat{\delta}}{2(\hat{\alpha} + \hat{\gamma})} Q(x_{j,i+1} - x_{j,i-1}) \end{aligned} \quad (9-a)$$

$$\begin{aligned} y_{i,j}^n &= \frac{\hat{\alpha}}{2(\hat{\alpha} + \hat{\gamma})} (y_{j-1,i} + y_{j+1,i}) + \frac{\hat{\gamma}}{2(\hat{\alpha} + \hat{\gamma})} (y_{j,i-1} + y_{j,i+1}) + \\ &\frac{0.5 \hat{\delta}}{2(\hat{\alpha} + \hat{\gamma})} F(y_{j+1,i} - y_{j-1,i}) + \frac{0.5 \hat{\delta}}{2(\hat{\alpha} + \hat{\gamma})} Q(y_{j,i+1} - y_{j,i-1}) \end{aligned} \quad (9-b)$$

Where

$$\hat{\alpha} = 0.25 (x_{i+1,j} - x_{i-1,j})^2 + (y_{i+1,j} - y_{i-1,j})^2 \quad (9-c)$$

$$\hat{\gamma} = 0.25 (x_{j+1,i} - x_{j-1,i})^2 + (y_{j+1,i} - y_{j-1,i})^2 \quad (9-d)$$

$$\hat{\delta} = \frac{[(x_{j+1,i} - x_{j-1,i})(y_{j,i+1} - y_{j,i-1}) - (x_{j,i+1} - x_{j,i-1})(y_{j+1,i} - y_{j-1,i})]}{16} \quad (9-e)$$

The steady-state governing equations (2-5) were solved by the finite-volume-method using Patankar's SIMPLE algorithm [Patankar, 1980]. A two-dimensional non-

uniformly collocated grid system was used. These equations can be written in a general transport equation as [Patankar, 1980]:-

$$\frac{\partial(\rho u \phi)}{\partial x} + \frac{\partial(\rho v \phi)}{\partial y} = \frac{\partial}{\partial x} \left[\Gamma_{\phi} \left(\frac{\partial \phi}{\partial x} \right) \right] + \frac{\partial}{\partial y} \left[\Gamma_{\phi} \left(\frac{\partial \phi}{\partial y} \right) \right] + S_{\phi} \quad (10)$$

This equation serves as a starting point for computational procedure in (FVM) [Ferziger and Peric, 1999]. The set of governing equations are integrated over the control volumes, which produces a set of algebraic equations. The SIMPLE algorithm is used to solve the coupled system of governing equations. The set of algebraic equations are solved sequentially. A second-order upwind

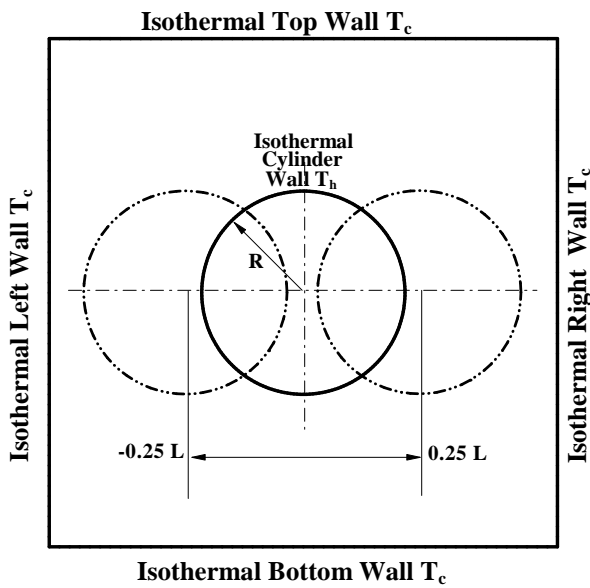


Fig. 1. Schematic diagram of the square enclosure with inner circular cylinder with coordinate system along with boundary conditions

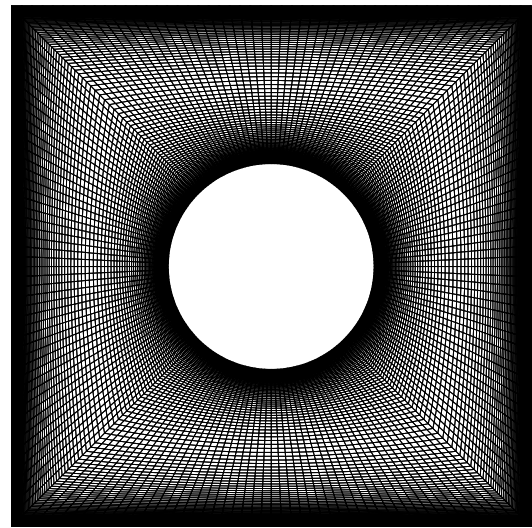


Fig. 2. A typical grid distribution (100 x 200) with non-uniform and non-orthogonal distributions for $\delta = 0$.

differencing scheme is used for the formulation of the convection contribution to the coefficients in the finite-volume equations. Central differencing is used to discretize the diffusion terms. The computation is terminated when the residuals for the continuity and momentum equations get below 10^{-5} and the residual for the energy equation gets below 10^{-8} . For the general curvilinear coordinates system (ξ, η) , the general transport equation (Eq.10) can be transformed to the following form [Patankar, 1980]:-

$$\frac{\partial}{\partial \xi} \left(\rho U_{co} \phi - \frac{a_1 \Gamma_{\phi}}{J} \frac{\partial \phi}{\partial \xi} \right) + \frac{\partial}{\partial \eta} \left(\rho V_{co} \phi - \frac{a_2 \Gamma_{\phi}}{J} \frac{\partial \phi}{\partial \eta} \right) = S_{NEW} \quad (11)$$

where (U_{co}, V_{co}) are the contravariant velocity components and $S_{NEW} = JS_{\phi} + S_N$ where S_N is the source term due to non orthogonal characteristic of grid system which disappear under orthogonal grid system. The transformation coefficients (a_1, a_2) are defined as [Patankar, 1980]:-

$$\left. \begin{aligned} a_1 &= \xi_x^2 + \xi_y^2 \\ a_2 &= \eta_x^2 + \eta_y^2 \end{aligned} \right\} \quad (12)$$

and the transformation metrics are calculated as follows:

$$\left. \begin{aligned} \xi_x &= \frac{y_\xi}{J} \\ \xi_y &= -\frac{x_\eta}{J} \\ \eta_x &= -\frac{y_\xi}{J} \\ \eta_y &= -\frac{x_\xi}{J} \end{aligned} \right\}$$

For the velocity field, the no-slip boundary conditions are imposed on the walls. The hot and cold wall temperatures of $\theta = 0$ and 1 are imposed on the walls of the square enclosure and the inner cylinder wall, respectively.

4. Validation of Numerical Results:

The mathematical model described above is solved using a finite volume approach. The equations are integrated over elementary control volumes that are located around each node of a mesh. The location of the nodes is calculated using a stretching function so that the node density is higher near the walls of the square enclosure and the inner circular cylinder. Fig. 2 shows the computational geometry in the (x - y) plane with a non-uniform grid distribution. The grids were non-uniformly distributed near the walls in order to account for the high gradients. The denser grid lines were uniformly distributed within the cylinder. In order to consider the variation of δ , the number of grid points used in the y direction is tuned to maintain the dense resolution near the walls and within the inner cylinder. Grid independence of the solution has been tested with additional simulations on much finer grids up to $301(x) \times 301(y)$ points. The difference in the results of Nusselt number obtained using the coarse and fine grids was less than 2% so a grid resolution of 201×201 along horizontal (x) and vertical (y) directions was employed in computations to be reported in the present study. For the purpose of the present numerical algorithm validation, the natural convection problem for a low temperature outer square enclosure and high temperature inner circular cylinder was tested. The calculated surface-averaged Nusselt numbers for the test case are compared with the benchmark values by Kim et al., 2008, and Moukalled and Acharya, 1996 as shown in Table 1. A general agreement between the present computation values and the previous values by Kim et al., 2008, and Moukalled and Acharya, 1996, are seen to be very well with a maximum deviation of about 2.2125%. Further validation was performed by using the present numerical algorithm to investigate the same problem considered by Kim et al., 2008 using the same flow conditions and geometries, which were reported for laminar natural convection heat transfer using the same boundary conditions but the numerical scheme is different. The comparison is made using the following dimensionless parameters : $Pr = 0.7$, $Ra = 10^3 - 10^6$ and $\delta = 0$. Excellent agreement was achieved between Kim et al., 2008, and the

present numerical scheme for both the streamlines and temperature contours inside the square enclosure with the inner cylinder along the horizontal centerline at $\delta = 0$ as shown in Fig.3. These validations make a good confidence in the present numerical model to deal with the other horizontal locations (δ 's) .

Table (1) Comparison of present surface-averaged Nusselt number with those of previous numerical studies

Maximum difference (%)	Mean Nusselt number at hot wall			Ra
	Moukalled and Acharya, 1996.	Kim et al., 2008	Present study	
-2.2125	3.331	3.414	3.4047	10^4
-0.96318	5.08	5.1385	5.12893	10^5
-0.1573	9.374	9.39	9.38875	10^6
0.57314	15.79	15.665	15.6995	10^7

5. Results and Discussion

The results are presented for a number of cases corresponding to $Ra = 10^3 - 10^6$ and horizontal position from $-0.25L$ to $0.25L$. The basic features of flow and heat transfer are analyzed with the help of isotherms and the streamlines patterns. Average Nusselt numbers are plotted to evaluate the overall heat transfer process.

5.1 Flow and Temperature Fields as a Function of δ

In general, the heated lighter fluid is lifted and moves upward along the hot surface of the inner cylinder toward upper surface until it encounters the cold top wall. Then the fluid becomes gradually colder and denser while it moves horizontally outward in contact with the cold top wall. Consequently, the cooled denser fluid descends along the cold side wall.

5.1.1 $Ra=10^3$

Fig. 4 shows the isotherms and streamlines for different location (δ) in horizontal centerline and $Ra=10^3$. For $Ra=10^3$, the heat transfer in the enclosure is mainly dominated by the conduction mode. Because of the conduction, the distribution of the flow and thermal fields in Fig.4, shows the symmetric shapes about the horizontal center line at $y=0$ for different location (δ) ($-0.25L$ to $0.25L$). When the cylinder moves to the right or to the left of the enclosure side wall, the size of the two vortex in the right, when the cylinder moves right, and in the left, when the cylinder moves left, reduced in size to a small vortex on the other hand in the reverse side the two vortices merge into a single vortex at ($\delta= 0.15L$ and $-0.15L$), because the enclosure can secure enough space to enlarge the circulation of the left and right of the inner cylinder. As (δ) becomes more negative or positive, the isotherms becomes denser in between the inner cylinder and the left or the right side wall of the square enclosure, where as they become coarser in the opposite region. Also, Fig. 4 shows that the isotherm and streamlines are similar, but reverse, when the inner cylinder change locations to the right or to the left of enclosure side wall, because of the change in locations are orthogonal with buoyancy force .

5.1.2 $Ra = 10^4$

Fig.5 shows the distribution of isotherms and streamlines for different position when $Ra=10^4$. As Ra increases to 10^4 , the effect of convection on heat transfer becomes larger than that at $Ra=10^3$. Thus, the distribution of flow and thermal fields in left and right column of Fig.5 for negative and positive δ value shows the asymmetric shapes about the horizontal center line at $y=0$, compared with that in Fig.4, when the $Ra=10^3$. When the inner cylinder goes to the left or to the right of the enclosure side wall, the isotherms are gradually distorted and the size of the thermal plumes on the left and the right of the inner cylinder becomes larger. The overall view of the Fig.5 shows that the distribution of isotherms and streamlines when $\delta = -0.25L$ to $0.25L$, have the same shape but reverse due to the change of the orthogonal position with buoyancy force for natural convection.

5.1.3 $Ra=10^5$

Fig. 6 shows the distribution of isotherms and streamlines for different δ s when $Ra=10^5$. When the inner cylinder moves horizontally to the right or the left side wall of the enclosure, the single vortex gradually separated to two vortex because of no enough space existent between the inner cylinder and the right or left side wall of the enclosure, also, the other vortex increase in size due to increase the space between the inner cylinder and the right or left side wall of enclosure. The distribution of the isotherms in the enclosure at $Ra=10^5$ is significantly different from that at the lower Rayleigh numbers because the buoyancy induced convection becomes more predominant than conduction.

When the inner cylinder moves to the right side wall of the enclosure, the pattern of isotherms and streamlines is the same that when the inner cylinder moves to the left side wall, but reverse. When the cylinder moves to right or left side wall, the isotherms squeezed from side and elongate from other side along the horizontal center line, because the distance between the inner cylinder and the right or the left side walls increase or decrease when the δ change from $-0.25L$ to $0.25L$.

5.1.4 $Ra=10^6$

The maps of isotherms and streamlines for different δ s when $Ra=10^6$ shows in Fig.7. At Rayleigh number equal to 10^6 , the magnitude of the velocity circulating in the enclosure increase and the isotherms are distorted more due to the stronger convection effects, leading to the stable stratification of the isotherms. As a result the thickness of the thermal boundary formed on the surfaces of the inner cylinder and the enclosure becomes thinner and the thermal gradients on the walls becomes larger when $Ra=10^6$, compared to those when $Ra=10^5$. When the position of inner circular cylinder change to the right or to the left side wall of the square enclosure, the ascending plume on the upper part of the inner cylinder incline, from center line of inner cylinder to the left or to the right corresponding with elongated vortices in the enclosure.

5.2 Surface Averaged Nusselt Number

Figs.8 and 9 shows the surface-averaged Nusselt number at the surface of the square enclosure and surface of the inner cylinder as a function of (δ), respectively, for different Rayleigh numbers. In general, the average Nusselt number of square enclosure and for inner cylinder increases with increasing Rayleigh number due to the increasing effect of convection. Also, the Nusselt increasing with change the position to the left and to the right side wall with same value due to perpendicularity between the change of position and the buoyancy force.

Fig.8 shows the surface average Nusselt number for cold square enclosure as a function of (δ) for different Rayleigh numbers. The average Nusselt number increase with change the position to the left or to the right side wall due to decrease the distance between the hot inner cylinder and the side wall of the enclosure and this leads to increase the thermal gradient on enclosure. The average Nusselt number $Ra=10^4$ closed to the average Nusselt number for $Ra=10^3$, due to high effects of conduction. Also, the effect of convection become high with increase Rayleigh, such as increase at $Ra=10^6$.

Fig.9 shows the surface average Nusselt number for heated inner circular cylinder, nearly, the same observation of Nusselt for square enclosure can be drawing to the hot circular cylinder, but the Nusselt number in case of a heated cylinder have values greater than that of the square enclosure because the inner circular cylinder is hot and have thermal gradient higher than of that for cold square enclosure.

6. Conclusions

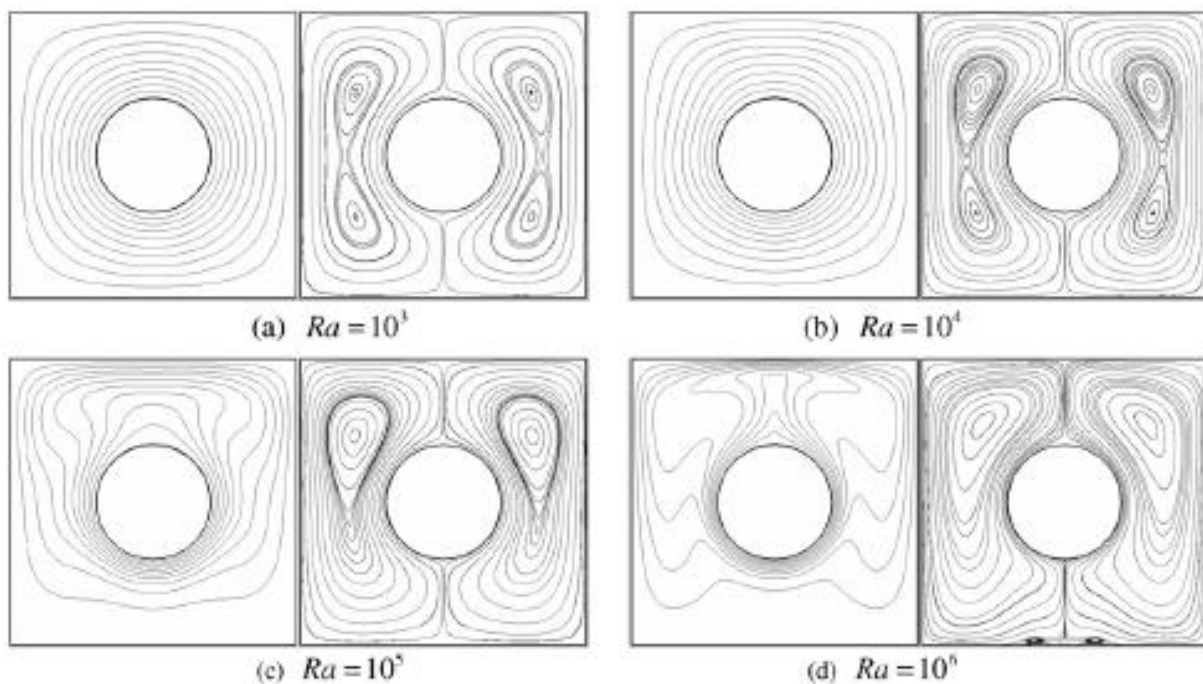
A numerical study has been carried out for two-dimensional natural convection problem in a cooled square cylinder. The finite volume method with SIMPLE algorithm was implemented to simulate the flow and heat transfer over an inner circular cylinder in general coordinates. A detailed analysis for the distribution of streamlines, isotherms and Nusselt number was carried out to investigate the effect of the locations of the heated inner cylinder on the fluid flow and heat transfer of Rayleigh numbers in the range of 10^3 to 10^6 .

For all Rayleigh numbers considered in the present study, the flow and thermal fields affects with change the position of the inner circular cylinder. The streamline in one side of the square enclosure have two vortices, for the side when distance small and single vortex for the side when the distance larger. The thermal plumes become denser when the (δ) change from (-0.25L to 0.25L) when compare with case of ($\delta=0$). The variation of the total surface-averaged Nusselt number of the enclosure as a function of (δ) for different Rayleigh numbers is similar to surface-averaged Nusselt numbers of the inner cylinder. When $Ra=10^3$ and 10^4 the Nusselt for enclosure and inner cylinder have a parabolic profiles with a minimum values at ($\delta=0$) and show a symmetric shape around ($\delta=0$). The value of average Nusselt for inner cylinder is larger than that of average Nusselt for square enclosure because the isotherms are formed more densely on the inner cylinder surface than that on the surfaces of the enclosure. Further, it could analyze the effect of the diagonal change of locations of heat circular cylinder immersed in rectangular enclosure filled with air, in future works, which is interesting and important in many engineer application.

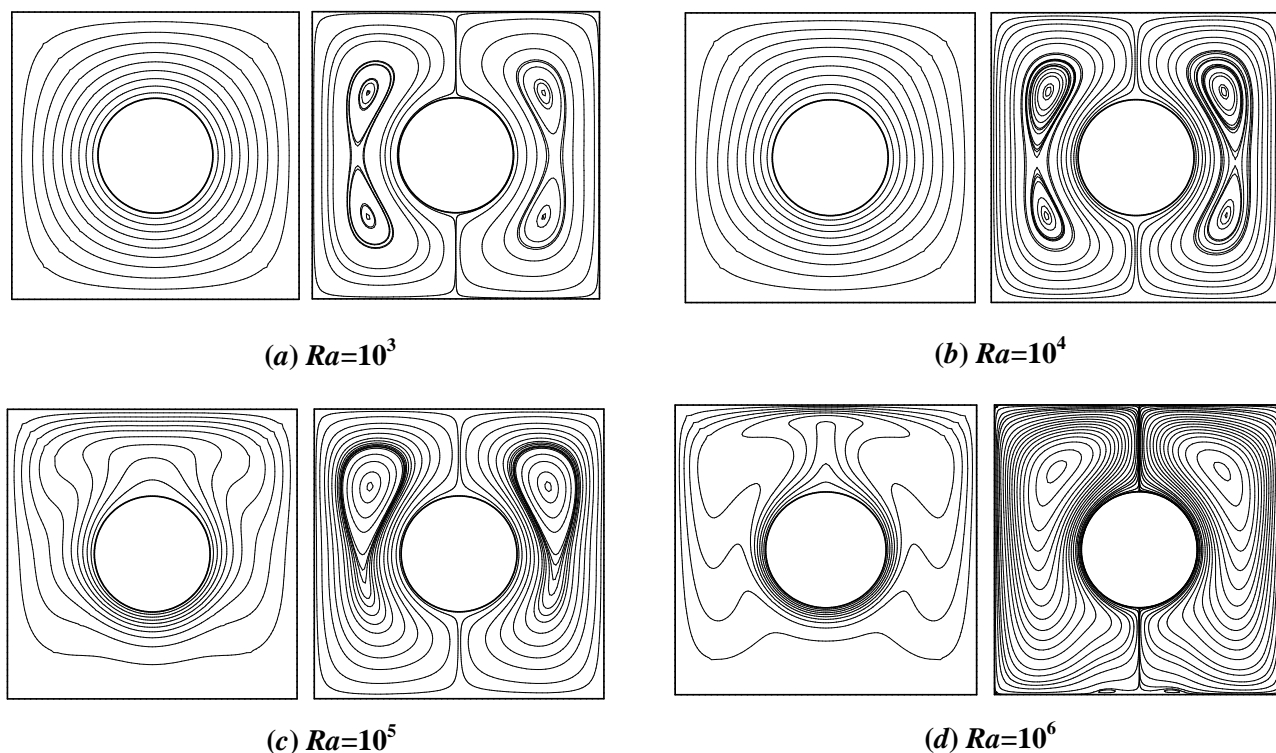
7. References

- Arpaci, P., and Larsen, P., 1984, "Convection Heat Transfer", Prentice-Hall.
- Asan, H., 2000, "Natural convection in an annulus between two isothermal concentric square ducts", International Communications in Heat Mass Transfer (27), pp:367-376.
- Cesini, G., Paroncini, M., Cortella, G., and Manzan, M., 1999, "Natural convection from a horizontal cylinder in a rectangular cavity", International Journal of Heat and Mass Transfer (42), pp:1801-1811.
- Ding, H., Shu, C., Yeo, K.S., and Lu, Z.L., 2005, "Simulation of a natural convection in eccentric annuli between a square outer cylinder and a circular inner cylinder using a local MQ-DQ method", Numerical Heat Transfer Part A (47), pp:291-313.
- Ferziger, J., and Peric, M., 1999, "Computational methods for fluid dynamics", 2nd edition Springer Verlag, Berlin Hedelberg.
- Ghaddar, N.K., 1992, "Natural convection heat transfer between a uniformly heated cylindrical element and its rectangular enclosure", International Journal of Heat and Mass Transfer (35), pp:2327-2334.
- Ghaddar, N.K., and Thiele, F., 1994, "Natural convection over a rotating cylindrical heat source in a rectangular enclosure", Numerical Heat Transfer Part A (26), pp:701-717.
- Kim, B.S., Lee, D.S., Ha, M.Y., and Yoon, H.S., 2008, "A numerical study of natural convection in a square enclosure with a circular cylinder at different vertical locations", International Journal of Heat and Mass Transfer, (51), pp:1888-1906.
- Kumar De, A., and Dalal, A., 2006, "A numerical study of natural convection around a square, horizontal, heated cylinder placed in an enclosure", International Journal of Heat and Mass Transfer (49), 4608-4623.

- Lacroix, M., 1992, "Natural convection heat transfer around two heated horizontal cylinders inside a rectangular cavity cooled from above", *Numerical Heat Transfer Part A* (21), pp:37–54.
- Moukalled, F., and Acharya, S., 1996, "Natural convection in the annulus between concentric horizontal circular and square cylinders", *Journal of Thermophysics Heat Transfer* (10) , pp:524–531.
- Patankar, S.V., 1980, "Numerical heat transfer and fluid flow" , Hemisphere Publishing Corporation, New York.
- Saha, A.K., 2000, "Unsteady free convection in a vertical channel with a built-in heated square cylinder", *Numer. Heat Transfer Part A* (38), pp:795–818.
- Sasaguchi, K., Kuwabara, K., Kusano, K., and Kitagawa, H., 1998, "Transient cooling of water around a cylinder in a rectangular cavity – a numerical analysis of the effect of the position of the cylinder", *International Journal of Heat and Mass Transfer* (41), pp:3149–3156.
- Shu, C., and Zhu, Y.D., 2002, "Efficient computation of natural convection in a concentric annulus between an outer square cylinder and an inner circular cylinder", *International Journal of Numerical Method in Fluids*, (38) , pp:429–445.
- Shu, C., Xue, H., and Zhu, Y.D., 2000, "Numerical study of natural convection in an eccentric annulus between a square outer cylinder and a circular inner cylinder using DQ method", *International Journal of Heat and Mass Transfer*(44) ,pp:3321–3333.
- Thomas, P. D. and Middlecoff, J. F., 1980, " Direct Control of The Grid Point Distribution In Meshes Generated by Elliptic Equations", *AIAA Journal* , Vol. 18, No. 6, pp: 652-656.
- Thompson, P. D. , Thamas, F. C. and Mastin, F., 1974, "Automatic Numerical Generation of Body- Fitted Curvilinear Coordinate System", *Journal of computational physics*, (15) , pp:299-319.



Kim *et al.*, 2008, Results



Present Results

Fig. 3. Comparison of the temperature contours and streamlines between the present work and that of Kim *et al.*, 2008, at $\delta = 0.0$ for four different Rayleigh numbers of (a) 10^3 , (b) 10^4 , (c) 10^5 and (d) 10^6

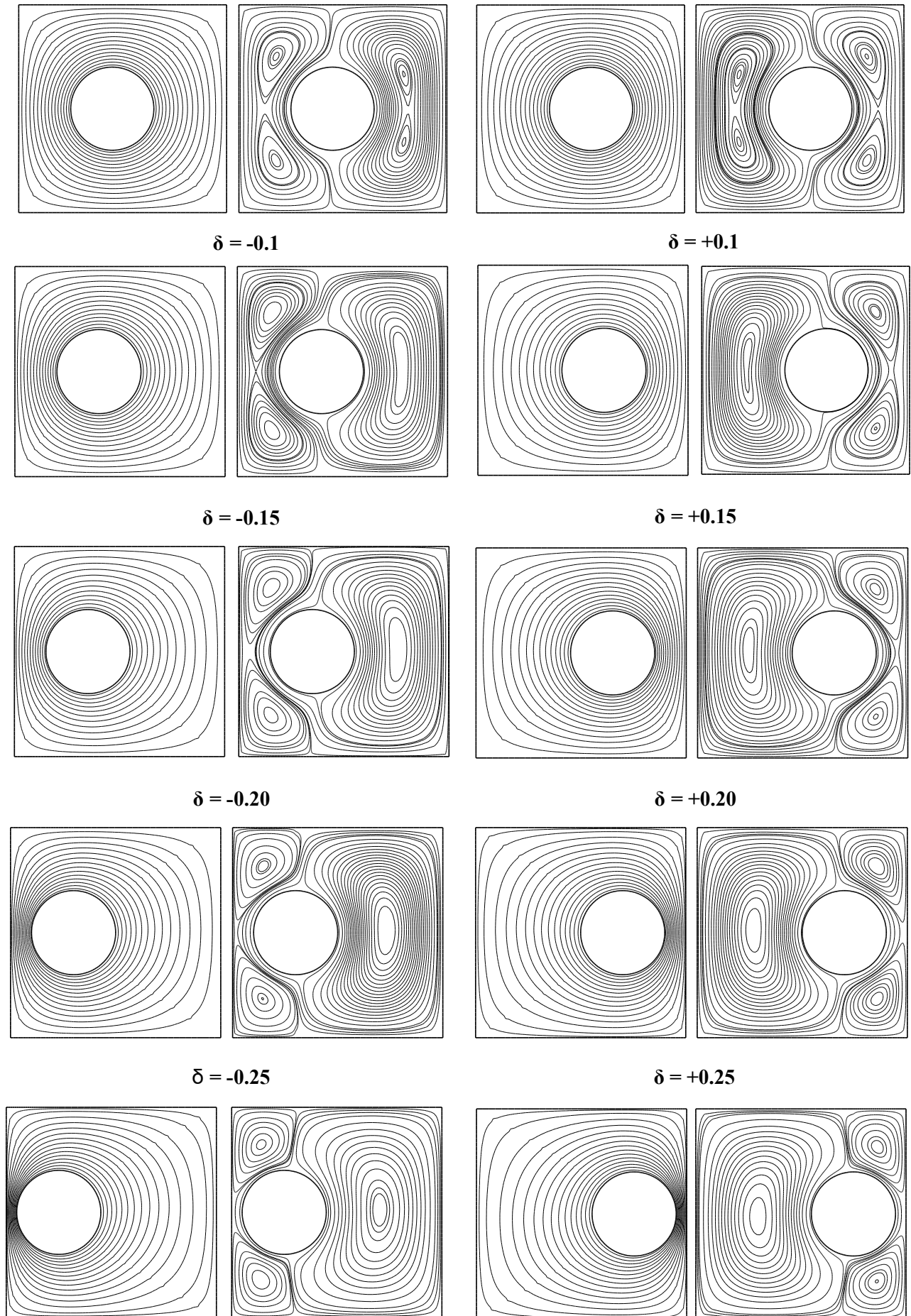


Fig. 4. Isotherms and streamlines for different δ s at $Ra=10^3$ (Contour values ranging from 0.1 to 1)

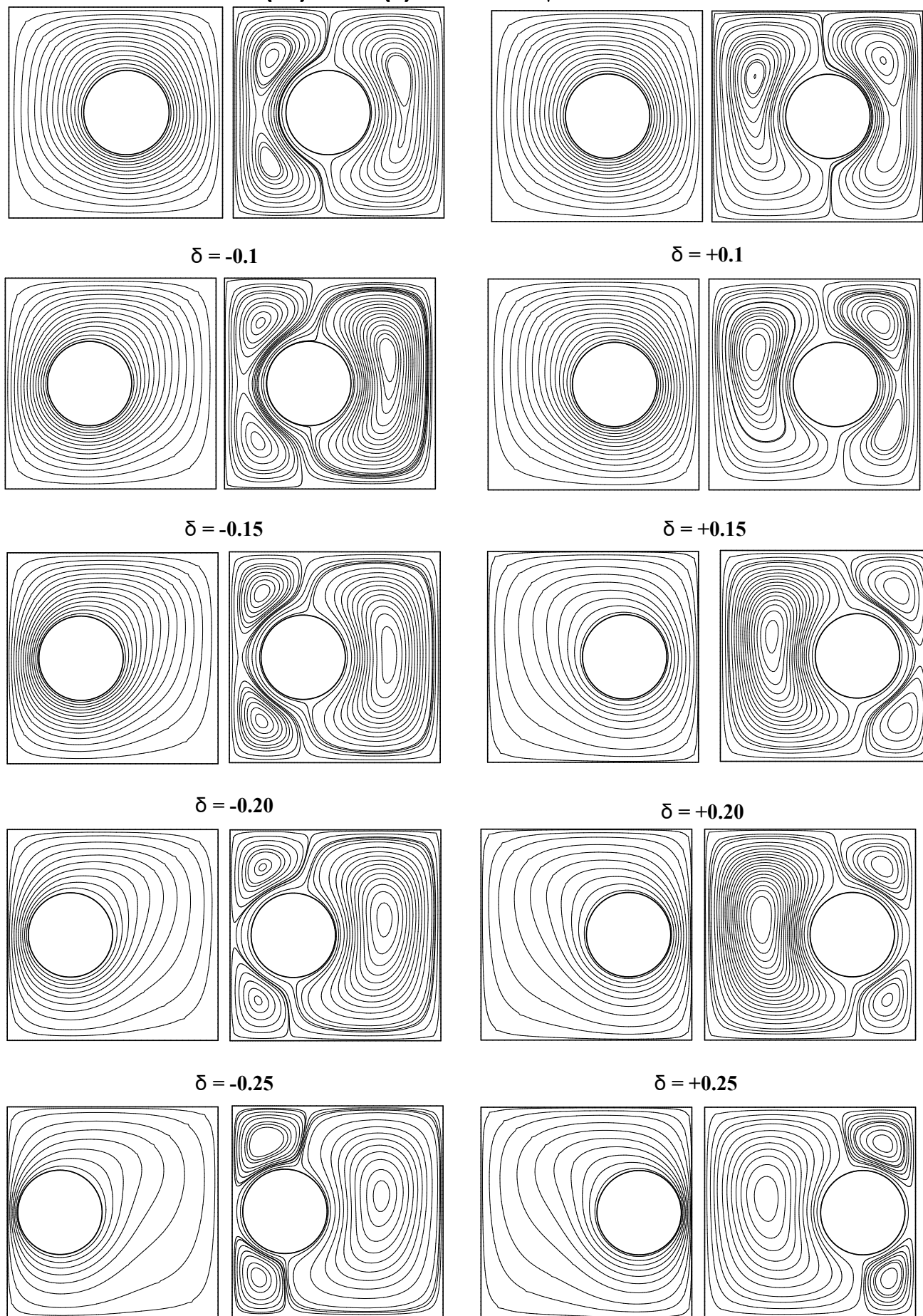


Fig. 5. Isotherms and streamlines for different δ s at $Ra=10^4$ (Contour values ranging from 0.1 to 1)

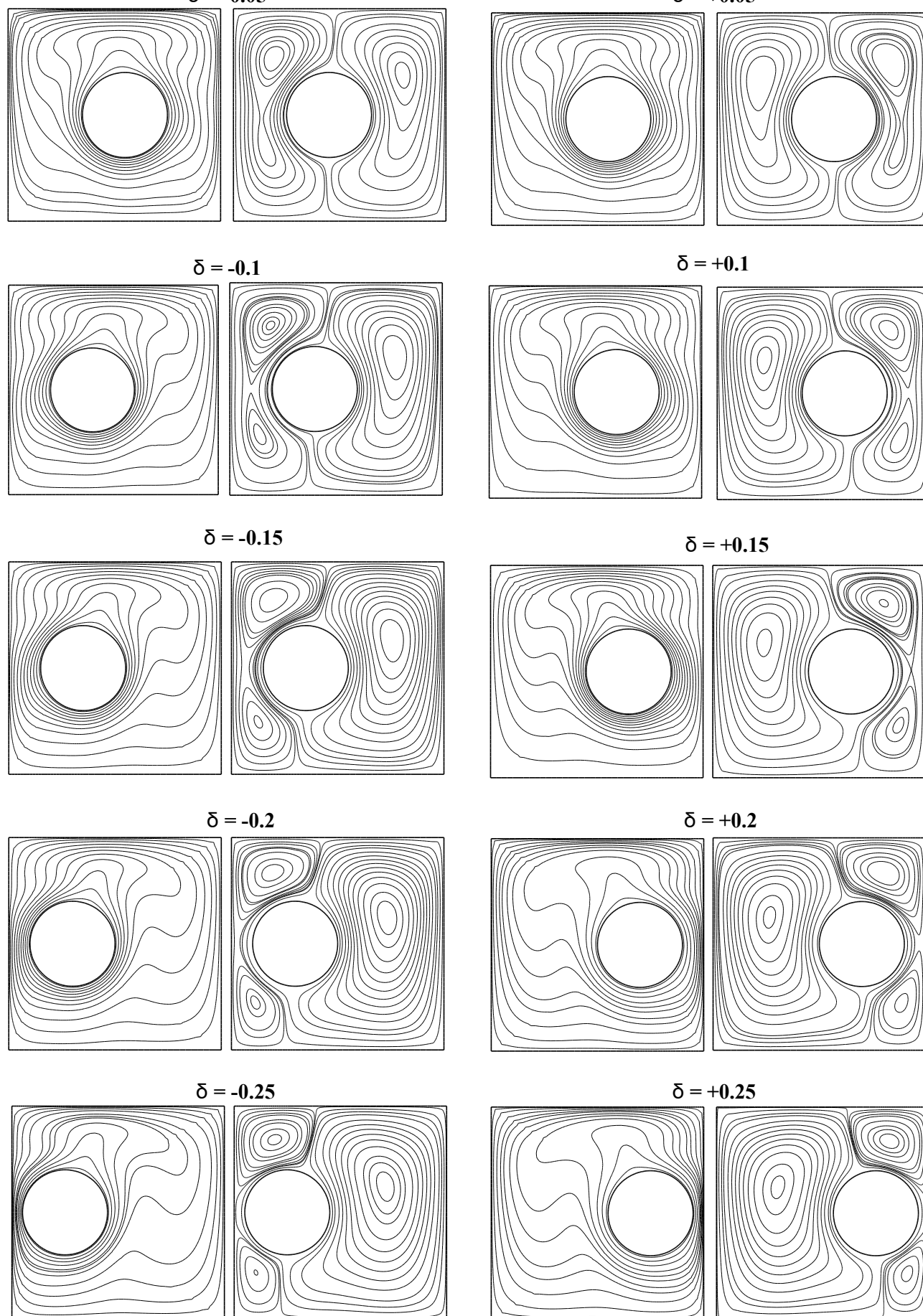


Fig.6. Isotherms and streamlines for different δ s at $Ra=10^5$ (Contour values ranging from 0.1 to 1)

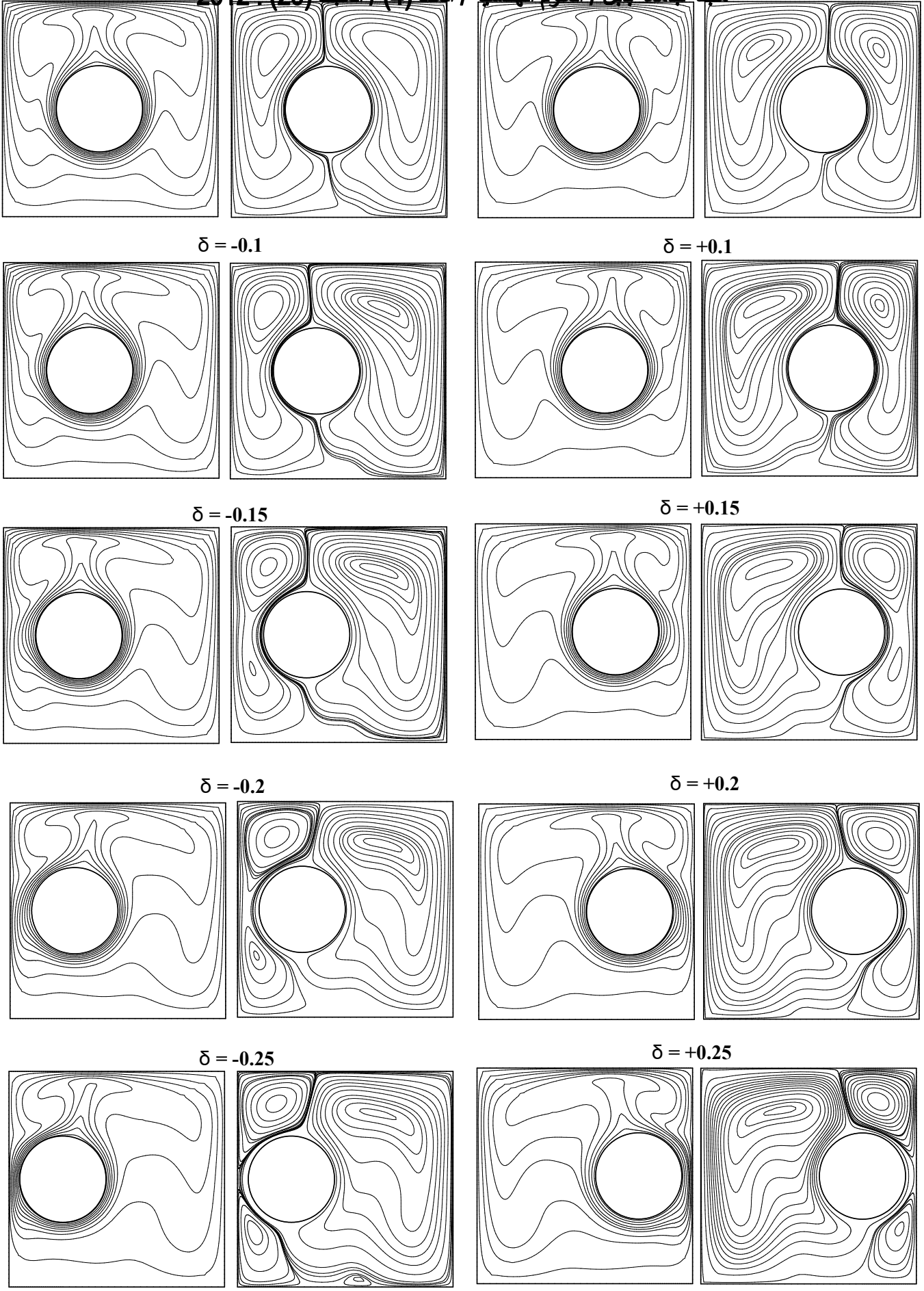


Fig. 7. Isotherms and streamlines for different δ s at $Ra=10^6$ (Contour values ranging from 0.1 to 1)

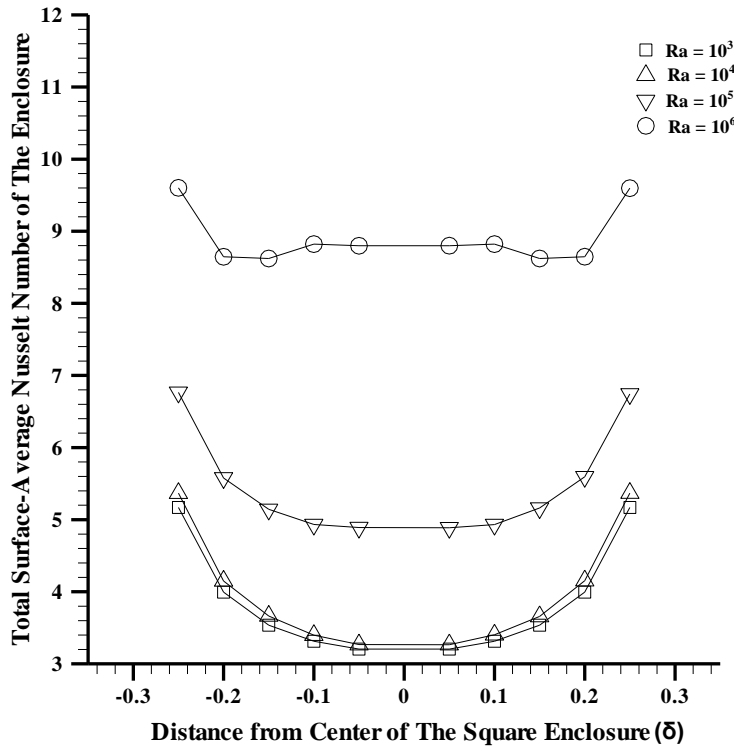


Fig. 8. Total surfaces-averaged Nusselt number of the cold square enclosure along the δ for The different Rayleigh numbers.

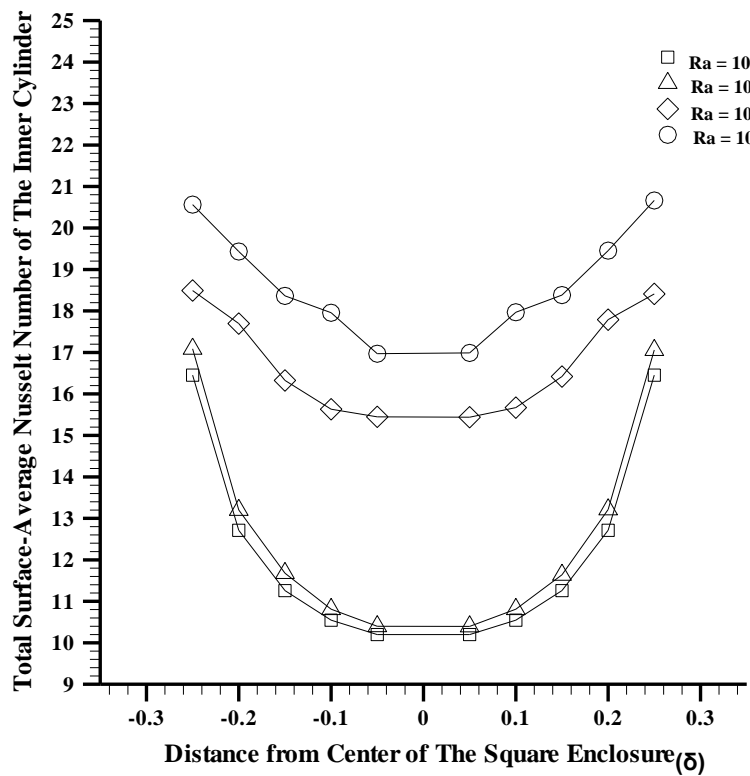


Fig.9. Total surfaces-averaged Nusselt number of the inner hot cylinder along the δ for the different Rayleigh numbers.